Memoirs of the Faculty of Science, Kyoto University, Series of Physics, Astrophysics, Geophysics and Chemistry, Vol. XXXIX, No. 1, Article 1, 1994

Earthquake Mechanisms and Its Implication for Tectonic Stress Field in the Southern Part of the North-South Seismic Belt in China

By

Jiren XU

Department of Geophysics, Faculty of Science, Kyoto University
Kyoto 606-01, Japan

(Received November 5, 1993)

Abstract

The southern part of the North-South Seismic Belt (NSB) in the central part of China is an active earthquake zone in the continental crust. The regional characteristics of stress field there have been analyzed detail based on mechanism solutions of 119 earthquakes from 1993 to 1991. The results show that the southern part of the NSB is a shallow earthquake zone where most earthquakes are caused by the strike-slip faulting. There is a systematic distribution of the directions of P- and T-axes in the western and the eastern regions of the southern part of the NSB. P- and T-axes in the western region are in the NE-SW direction and in the NW-SE direction. P- and T-axes in the eastern region are in the NW-SE direction and in the NE-SW direction, respectively. The average directions of P-axes in the western and the eastern regions show a pattern of a reversal "V". The boundary between these two regions coincides with that between the Tibetan plateau and the Yangtze crustal block. It suggests that the tectonic forces from the Himalayan collision zone between the Indo-Australian and the Eurasian plates and from the eastern coast collision zone in Taiwan between the Philippine Sea and the Eurasian plates are transmitted to the western and eastern regions of southern part of the NSB, respectively, and control the stress field there. There are the rotation of directions of P- and T-axes from southern to northern subregions in the western region and the eastern region. It can be inferred northward motions of the Yangtze crustal block and the Tibetan plateau in the southern subregions mutually encountering there. The strong obstruction of Qinling mountains changes the direction of regional stress field in the northern subregions.

1. Introduction

One of characteristics of the seismicity in the continental part of China is that spatial distribution of shallow earthquakes can be divided into two main parts, the eastern part and the western part, from seismological viewpoint. Boundary between them is called the North-South Seismic Belt (NSB) which is also called the North-South-Trending Belt by some authors (Editorial board of the atlas on the lithospheric dynamics of China State Seismological Bureau, 1987). The NSB is a large-scale tectonic zone with N-S trend between longitudinal lines of 98°E and 105°E, which stretches over 2,000 km from north to south, beginning from the Dengkou region of the Inner Mongol Autonomous region, through the Yinchuan, Haiyuan in Ningxia Autonomous region, Songpang, Luhuo in Sichuan province and the southern part of

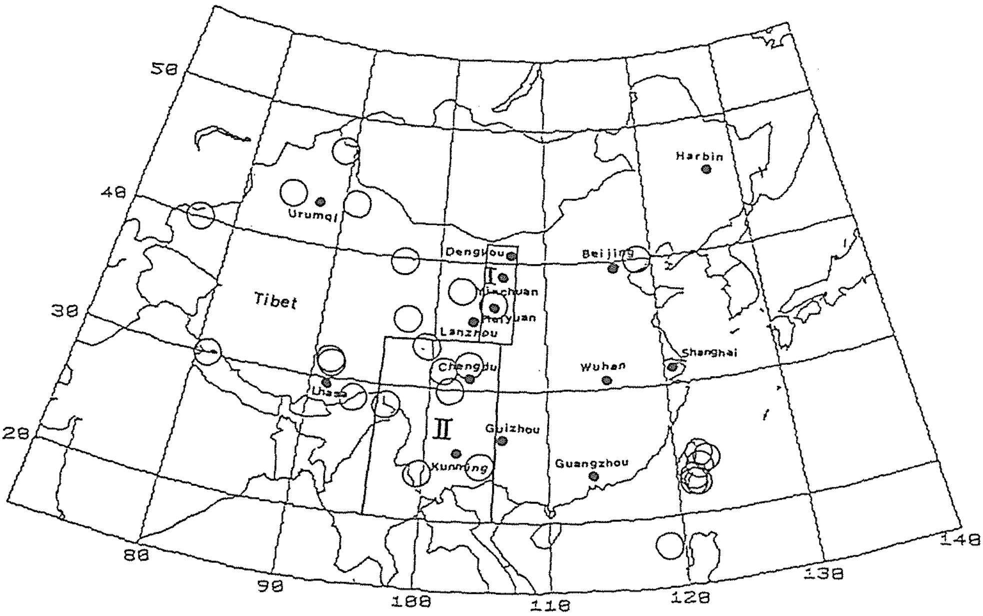

1a

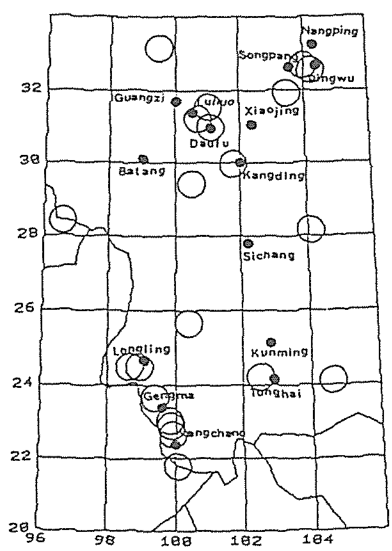

1b

Fig. 1(a). Distribution of epicenters of shallow earthquakes (M≧7.5) from 1900 to 1991 in China and the ranges of the northern part (I) and the southern part (II) of the NSB. The latter if studied in the present paper. (b) Distribution of epicenters of earthquakes (M≧7.0) from 1900 to 1991 in the southern part of the NSB.

Yunnan province, to Myanmar (Fig. 1(a)). Its width increases from the northern segment where the width is about 200 km to the southern segment where that is about 600 km. Many large earthquakes concentrate in this long region, for example, the 1920 Haiyuan earthquake (M=8.6) which is the largest inland earthquake recorded in China, the 1933 Diexi earthquake (M=7.5) which made more than 10 earthquake lakes in the epicentral region, the 1955 Kangding earthquake (M=7.5), the 1970 Tonghai earthquake (M=7.7) which generated a earthquake fault longer than 60 km, the 1973 Luhuo earthquake (M=7.6) and the 1976 Songpang earthquakes (M=7.2, 7.2) (see Fig. 1(a)).

The NSB can be divided into two parts, the northern part and the southern part. The boundary between the northern part and the southern part of the NSB is in the northern side of the Songpang region in Sichuan province (see Fig. 1(a)). After the 1954 Mingqin earthquake (M=7.3), no large earthquakes (M≧7) occurred and the seismic activity has been low in the northern part of the NSB. But in its southern part, the high seismic activity has continued up to the present (Zhao et al., 1988, Wang et al., 1976) (see Fig. 1(b)). In November, 1988, the M 7.6 earthquake occurred in the Langchang-Gengma region in Yunnan province, which is the largest one in the southern part of the NSB in the last active period. On April 23, 1992, two earthquakes with magnitudes 6.7 and 6.9 occurred in the boundary between China and Myanmar located in the southern part of the NSB.

Fig. 1(a) shows the epicentral distribution of earthquakes with magnitude more than or equal to 7.5 in China from 1900 to 1991. The NSB is easily identified in Fig. 1(a). Fig. 1(b) shows the epicentral distribution of earthquakes with magnitude more than or equal to 7.0 in the southern part of the NSB from 1900 to 1991, where 21 large earthquakes occurred and the active seismicity is recognized during this period.

The southern part of the NSB has not only the active seismicity but also the complicated characteristics of seismotectonics comparing with those of other seismically active zones in China. Many significant characters of seismicity and stress field in the southern part of the NSB have been reported. Kan et al. (1977) have pointed out that the strong collision of the Indo-Australian plate through the Tibetan plateau made a tectonic block with rhombus shape in Sichuan and Yunnan provinces in the southern part of the NSB move southeastward relatively to the neighbor regions and controls the earthquake-generating stress field. Xu et al. (1987) deduced mean directions of principal axes of stresses from initial motion of P-wave of microearthquakes occurred from 1975 to 1984 in the region from 23°N to 40°N of the NSB. The result indicated that both maximum compressional axes (P-axes) and maximum tensile axes (T-axes) are horizontal and azimuths of P-axes rotates from NE-SW in the northern part of NSB, through E-W in the middle part of NSB, to NNW-SSE or near N-S in the southern part of the NSB. Peltzer and Tapponnier (1988) investigated the processes which governed the formation and evolution of large strike-slip faults in the Asian continent due to the intrusion of Indian peninsular into the Himalayan mountains by an experimental simulation under the free boundary conditions in the eastern and southeastern edges of Asian continent. The result suggested that strong compressive force by the northward moving Indo-Australian plate controlled the tectonic stress field in the southern part of the NSB. In order to clarify the seismotectonic nature in the continental part of China, it is necessary to study the locality of characteristics of stress field in the southern part of the NSB in detail.

Many large earthquakes occurred in the southern part of the NSB in recent years make it possible to study the stress field and the seismotectonics in this region using new source mechanism solutions. Characteristics of the earthquake-generationg stress field in the southern part of the NSB and its tectonic implication are discussed in this study using these solutions.

2. Data

Focal mechanism solutions of 119 earthquakes are used in this analysis to discuss the dynamic characteristics of stress field. The author newly determined 21 focal mechanism solutions in the present study based on data of the Bulletins of the International Seismological Center from 1971 to 1980. Data of events (M>5.5) from 1981 to 1990 referred from solutions of centroid-moment tenors (Dziewonski et al. 1983(a), 1983(b), 1983(c), 1985(a), 1985(b), 1986(a), 1986(b), 1987(a), 1987(b), 1989(a), 1989(b), 1990(a), 1990(b), 1990(c), 1991) were also used in the present analysis. Some important focal mechanism solutions in China including the 1933 Diexi earthquake (Sichuan province Seismological Bureau, 1983), the 1989 Xiaojin earthquake (M=6.6) (Xu, 1991) and the 1991 Xiaojin earthquake (M=5.2) (Xu, 1991) were changed from solutions of projection of upper hemisphere to ones of projection of lower hemisphere and to compare with those reported by other authors. Solutions of almost all main earthquakes with magnitude more than or equal to 4.8 from 1933 to 1991 are collected and confirmed. These convincing data were used in this study.

3. Characteristics of the Stress Field in the Southern Part of the NSB

The southern part of the NSB is a typical continental earthquake zone. All earthquakes here are shallow events whose depths are less than 70 km. Epicentral distribution of 119 earthquakes analyzed in the present study is listed in Table 1 and is shown in Fig. 2. Depths of almost all events expect those in the Myanmar region are less than 42 km in the crust.

Fig. 3 and Fig. 4 show horizontal projection of P-axes and T-axes of focal mechanism solutions of 119 shallow earthquakes in the region analyzed, respectively. Directions of P-axes show quite different distribution in the western region and the eastern region of the southern part of the NSB. Regular distribution of the principal stress axes exists in the western region and the eastern region in the southern part of the NSB, respectively. Most P-axes in the western region are in the NE-SW direction, except some events in the eastern part of Myanmar where P-axes lie nearly in the E-W direction. Most P-axes in the eastern region lie in the NW-SE direction, except some events whose P-axes lie nearly in the E-W direction in the Songpang region (104°E, 33°N), which is the northern end of the southern part of the NSB. Fig. 4 also shows the

Table 1. List of earthquake mechanism solutions used in this study

Date	Origin Time	Lat. (°N)	Long. (°E)	Depth (km)	M	N-axes Az.	N-axes Pl.	P-axes Az.	P-axes Pl.	T-axes Az.	T-axes Pl.
1933 8 25	15:50	31 60.0	103 42.0	0	7.5	79	58	232	29	329	13
1933 8 25	19:38	31 42.0	103 24.0	0	5.0	158	74	273	7	5	14
1950 8 15	14: 9	28 24.0	96 42.0	33	8.5	83	58	186	8	281	31
1955 4 14	9:29	29 60.0	101 54.0	33	7.5	303	68	122	22	33	0
1955 6 7	8:48	26 30.0	101 6.0	33	6.0	48	72	150	4	242	18
1955 9 23	23: 6	26 18.0	101 54.0	33	6.8	226	80	345	5	75	9
1958 2 8	7:23	31 30.0	104 0.0	0	6.2	186	90	96	0	180	90
1959 2 14	14:25	27 60.0	97 0.0	33	5.6	59	37	200	46	312	21
1960 11 9	18:43	32 48.0	103 42.0	6	6.8	295	69	81	18	175	11
1961 6 12	1:25	21 36.0	106 0.0	28	5.0	270	80	102	10	11	2
1961 6 27	15: 3	27 48.0	99 42.0	5	6.0	154	0	64	25	244	65
1962 2 27	14:34	27 36.0	101 54.0	33	5.5	356	65	122	15	218	19
1962 6 24	9:21	25 18.0	101 6.0	17	6.2	232	0	322	30	142	60
1963 4 23	17:55	25 48.0	99 30.0	20	6.0	52	85	210	5	300	2
1964 2 13	18: 3	25 36.0	100 36.0	24	5.4	29	58	132	8	227	31
1964 11 20	14:34	25 12.0	101 24.0	33	5.0	243	84	18	4	108	4
1965 5 24	0: 5	24 6.0	102 36.0	8	5.2	44	72	153	6	245	17
1965 7 3	19:26	22 24.0	101 36.0	15	6.1	353	69	164	21	255	3
1965 9 22	0: 0	20 36.0	99 24.0	11	6.1	351	76	216	10	125	10
1966 1 31	10:35	27 48.0	99 42.0	8	5.5	94	54	325	25	223	25
1966 2 5	23:12	26 12.0	103 12.0	5	6.5	274	80	123	9	33	5
1966 9 18	22:15	22 36.0	102 18.0	11	5.6	19	55	198	35	288	1
1966 9 19	13: 3	23 48.0	97 54.0	33	5.4	347	69	214	15	120	15
1966 9 23	5:54	26 18.0	104 30.0	6	5.0	208	68	298	0	28	22
1966 9 28	22: 0	27 18.0	100 24.0	6	6.4	359	34	183	56	90	1
1967 1 24	22:45	30 12.0	104 6.0	4	5.5	122	67	285	22	18	6
1967 5 5	8: 8	29 18.0	103 42.0	30	4.8	321	64	221	5	129	26
1967 8 30	19:18	31 42.0	100 20.0	35	6.0	100	82	249	7	339	4
1968 3 3	0:17	29 54.0	100 12.0	31	5.7	225	0	315	20	135	70
1968 3 16	20:26	25 18.0	101 6.0	33	5.1	349	48	79	0	168	42
1969 2 9	23:34	21 60.0	101 24.0	33	5.4	26	64	170	22	266	14
1969 7 2	0: 0	20 60.0	99 30.0	33	5.3	326	73	204	9	112	14
1970 1 5	1: 0	23 60.0	102 42.0	13	7.7	331	71	155	19	64	1
1970 2 7	6:10	22 54.0	100 48.0	17	6.0	99	66	357	5	265	23
1970 2 24	10: 7	30 36.0	103 12.0	15	6.2	42	23	312	0	222	67
1970 7 31	13:10	28 32.0	103 36.0	12	5.4	16	70	280	2	189	20
1970 9 5	21:37	32 6.0	101 18.0	20	5.5	9	73	262	5	170	16
1970 11 8	17:15	32 6.0	101 6.0	33	5.5	254	77	357	3	88	13
1970 11 18	1:59	25 12.0	101 54.0	33	5.0	234	81	336	2	67	9
1971 4 28	23:32	22 54.0	101 0.0	15	6.7	335	37	239	8	140	52
1971 5 30	15:44	25 6.0	96 24.0	15	6.4	145	74	261	7	353	14
1971 5 31	5:13	25 12.0	96 30.0	22	6.3	86	74	238	14	330	7
1971 8 16	4:58	28 54.0	103 36.0	16	5.8	288	56	126	33	30	8
1972 1 23	10: 5	23 30.0	102 30.0	33	5.5	345	37	227	32	109	36
1972 4 8	17:33	29 24.0	101 48.0	15	5.2	70	57	316	15	218	29
1972 7 7	0: 0	20 30.0	98 6.0	27	5.7	318	41	51	3	145	49
1972 9 27	0: 8	30 19.0	101 38.0	0	5.0	311	69	99	18	193	10
1972 9 29	16:21	30 24.0	101 35.0	3	5.1	145	62	271	17	7	21
1972 9 30	4:24	30 10.0	101 35.0	22	5.8	68	80	265	10	174	3
1973 2 6	18:37	31 24.0	100 36.0	17	7.9	322	86	78	2	168	4
1973 2 7	16: 6	31 30.0	100 20.0	35	5.9	15	29	180	60	282	7
1973 3 24	3:14	31 42.0	100 12.0	20	5.6	179	79	26	10	295	5
1973 5 8	18: 1	32 60.0	104 1.0	12	5.1	176	79	292	5	22	10
1973 6 1	21: 2	24 45.0	98 28.0	0	5.0	118	48	231	19	336	35
1973 6 29	5:29	28 46.0	103 40.0	20	5.5	140	54	293	33	31	13
1973 8 2	16:58	27 54.0	104 36.0	26	5.4	269	74	153	7	61	14
1973 8 11	15:15	32 54.0	104 0.0	8	6.5	26	29	119	5	220	60
1973 8 16	11:58	22 54.0	101 6.0	10	6.3	150	0	180	90	60	0
1973 9 9	10:13	31 42.0	99 48.0	32	5.8	145	74	29	7	297	14
1973 9 9	10:42	31 37.0	99 59.0	21	5.5	205	61	13	29	106	5

Table 1. List of earthquake mechanism solutions (continue)

Date	Origin Time	Lat. (°N)	Long. (°E)	Depth (km)	M	N-axes Az. Pl.	P-axes Az. Pl.	T-axes Az. Pl.
1974 1 16	6:50	32 54.0	104 6.0	18	5.7	186 68	284 4	16 22
1974 5 11	3:25	28 12.0	104 6.0	14	7.1	353 84	92 1	182 6
1974 6 5	8: 2	29 24.0	99 36.0	20	5.2	112 82	222 3	312 8
1974 6 15	18:19	31 36.0	100 0.0	13	5.0	325 75	231 1	140 15
1974 9 23	0: 0	33 48.0	102 36.0	11	5.6	326 71	127 18	218 6
1974 9 23	14:51	33 41.0	102 23.0	33	5.0	306 68	168 17	73 14
1974 11 17	0:25	32 60.0	104 6.0	33	5.7	37 51	138 9	236 38
1975 1 15	19:34	29 24.0	101 48.0	29	6.2	54 66	319 2	228 24
1975 5 30	17:44	26 42.0	97 0.0	30	6.4	296 0	206 40	26 50
1975 6 3	3:23	26 35.0	96 57.0	9	5.4	346 51	164 40	254 1
1975 12 1	2:22	27 14.0	100 25.0	20	5.0	331 25	202 53	74 26
1976 5 29	20:23	24 30.0	98 42.0	20	7.6	322 82	187 6	97 6
1976 6 9	0:20	24 56.0	98 44.0	13	5.6	48 72	205 18	288 9
1976 8 12	23:26	26 36.0	97 0.0	27	6.2	180 0	90 30	270 60
1976 8 16	22: 6	32 36.0	104 6.0	15	7.2	203 57	94 12	357 30
1976 8 19	20:49	32 54.0	104 18.0	15	5.9	37 66	298 4	207 24
1976 8 22	5:49	32 36.0	104 24.0	21	6.7	42 31	306 9	202 57
1976 8 23	11:30	32 30.0	104 18.0	23	7.2	188 25	279 1	11 65
1976 9 1	1: 6	32 26.0	104 10.0	29	5.0	151 62	258 9	353 26
1976 9 3	17:57	27 48.0	100 12.0	33	5.5	332 57	118 28	216 16
1976 9 20	22:45	32 46.0	104 8.0	42	5.0	31 50	293 7	197 39
1976 11 7	2:50	27 30.0	101 6.0	29	6.9	173 60	347 30	78 3
1976 12 13	14:36	27 18.0	101 12.0	17	6.4	76 69	333 5	241 20
1978 5 30	3:57	32 51.0	104 19.0	42	4.8	78 84	246 6	336 1
1978 7 13	5:49	31 55.0	102 55.0	33	5.4	102 35	305 53	200 12
1979 3 29	7: 7	32 26.0	97 16.0	0	5.4	144 83	234 0	324 7
1979 11 25	2:40	25 13.0	96 19.0	32	5.0	116 79	237 6	329 8
1979 12 21	6:31	27 6.0	97 2.0	32	5.5	124 0	214 35	34 55
1980 2 2	12:29	27 49.0	101 22.0	33	5.3	324 73	170 16	78 7
1981 1 23	21:13	30 56.0	101 6.0	10	5.7	272 70	97 20	6 2
1982 6 15	23:24	31 40.0	99 42.0	55	5.5	50 67	244 22	152 5
1982 6 16	7:24	31 50.0	99 51.0	17	6.0	252 81	50 8	141 3
1983 6 24	7:18	21 43.0	103 52.0	25	6.1	163 77	338 13	69 1
1984 4 23	22:29	21 47.0	99 38.0	17	5.9	141 65	38 6	305 24
1984 11 28	10:29	26 40.0	96 49.0	49	5.8	9 51	264 12	165 36
1985 4 18	5:52	25 23.0	102 38.0	10	5.7	172 56	317 29	57 16
1985 9 5	18:30	25 17.0	98 14.0	61	5.0	110 65	237 16	333 19
1986 3 13	8:41	25 27.0	101 1.0	15	5.4	342 6	87 69	250 21
1986 11 1	5: 2	25 32.0	96 55.0	70	5.4	176 28	270 7	13 61
1988 9 3	12:52	29 57.0	97 23.0	15	5.2	262 9	31 76	170 11
1988 11 6	13: 3	22 60.0	99 41.0	15	6.1	90 77	198 4	289 13
1988 11 7	2:40	23 23.0	99 25.0	15	4.9	156 39	65 2	333 51
1988 11 15	10:28	22 48.0	99 14.0	15	5.1	64 70	196 14	290 14
1988 11 27	4:17	22 42.0	100 10.0	15	5.0	134 58	25 11	289 29
1988 11 30	8:13	22 9.0	99 32.0	15	5.6	247 75	31 12	122 9
1989 1 18	18:22	29 53.0	100 8.0	15	5.0	240 46	90 40	347 15
1989 2 12	7:55	26 11.0	96 50.0	33	5.0	344 52	246 6	151 37
1989 3 1	3:25	21 37.0	98 18.0	58	5.1	124 76	27 2	297 14
1989 4 15	20:34	29 55.0	99 22.0	15	6.2	78 8	323 72	171 16
1989 4 25	2:13	29 54.0	99 25.0	15	6.1	264 16	59 73	172 7
1989 5 3	5:53	29 60.0	99 41.0	15	6.0	260 18	67 71	169 4
1989 5 3	15:41	29 50.0	99 26.0	15	5.9	91 0	180 90	181 0
1989 5 7	0:38	23 28.0	99 39.0	15	5.3	103 72	201 3	292 18
1989 7 21	3: 9	29 47.0	99 32.0	15	5.5	89 22	238 65	355 12
1989 9 22	2:25	30 52.0	102 50.0	15	6.0	20 9	285 29	125 60
1989 9 28	21:52	20 19.0	99 4.0	15	5.4	170 72	33 14	300 12
1989 9 30	18:19	20 16.0	99 14.0	15	5.3	129 73	308 17	38 0
1990 3 8	18:57	25 7.0	96 37.0	57	5.5	143 71	256 8	349 17
1991 2 18	17: 6	31 25.0	102 23.0	10	5.2	213 65	116 4	24 25

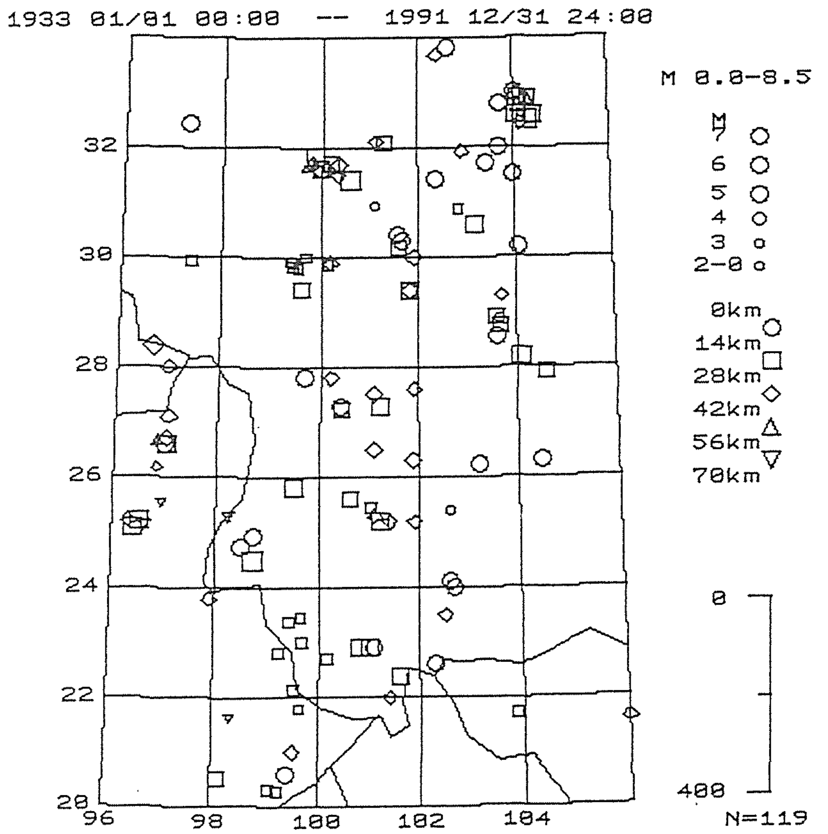

Fig. 2. Distribution of epicenters of 119 shallow earthquakes (4.8≦M≦8.5, depth less than 70 km) with mechamism solutions from 1933 to 1991 in the southern part of the NSB.

distribution of T-axes in the western region and in the eastern region in the southern part of the NSB. Most T-axes in the western region lie in the NW-SE direction and most T-axes in the eastern region are in the NE-SW direction. Some T-axes in the Myanmar region and the northern end of southern part of NSB lie in the N-S direction. The boundary dividing the pattern of distribution of the principal stress axes of focal mechanism is drawn by a complicated curve.

Based on directions of P-axes and T-axes, the southern part of the NSB can be zoned into seven subregions. They are, from south to north, subregions W1, W2 and W3 in the western region, and subregions E1, E2, E3 and E4 in the eastern region as shown in Fig. 5. In order to observe regional characteristics in detail, P-, T- and N-axes (Null vector) of focal mechanism solutions in each subregion were projected on the lower hemisphere using Wulff's net. Fig. 6 and Fig. 7 show the projections of three subregions (W1, W2 and W3) in the western region and in four subregions (E1, E2, E3 and E4) in the eastern region, respectively.

In Fig. 6, it can be seen that most P-axes of W1 are horizontal in the NE-SW direction, T-axes are horizontal in the NW-SE direction and N-axes concentrate around

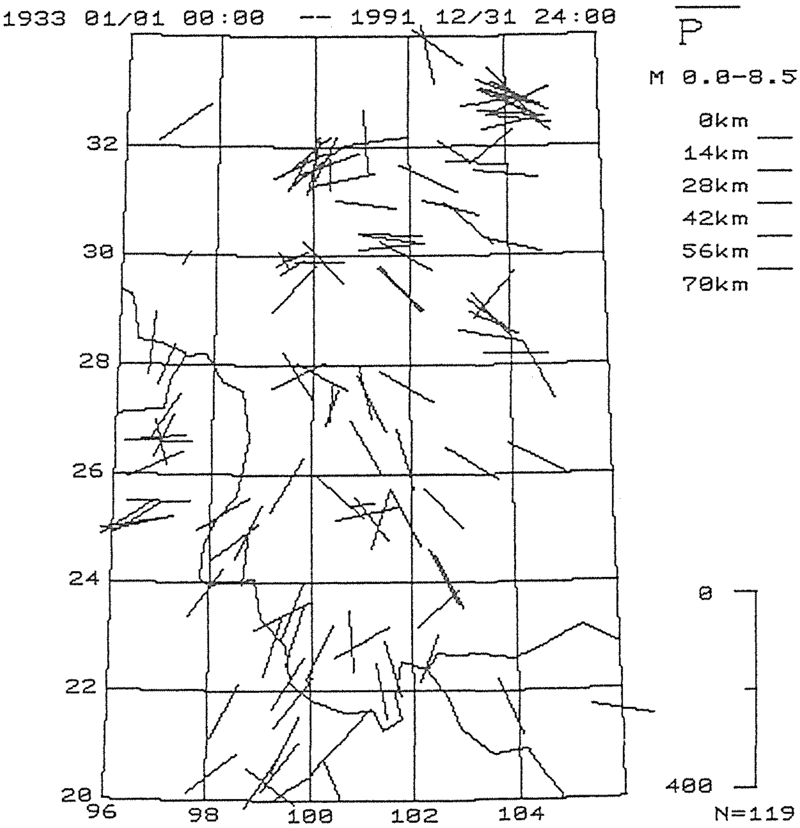

Fig. 3. Distribution of P-axes of the mechanism solutions of 119 earthquakes. It shows the different direction distributions in the western region and eastern region of the southern part of the NSB.

the vertical direction. So that the earthquake-generating stress field in the subregion W1 (the southwestern part of Yunnan Province) is characterized by NE-SW compression, NW-SE extension and the vertical null vector. It causes the strike-slip faulting type earthquakes. P-, T- and N-axes in the subregion W2 (the border area among Yunnan province, Sichuan province, Tibet of China and Myanmar) show somewhat different from those in the subregion W1. Some P-axes there are around the vertical direction, some in the NE-SW direction. T-axes there lie in the NNW-SSE direction. Such stress field causes normal faulting type earthquakes. In the subregion W3 located in the northwestern part of the Sichuan province, P-axes are horizontal in the ENE-WSW direction, T-axes are in the NW-SE direction and N-axes are concentrated around the vertical direction. This is also a subregion where strike-slip faulting earthquakes occur. In Fig. 6, the direction of P-axes seems to rotate from NNE-SSW to ENE-WSW from the subregion W1 to the subregion W3. T-axes also rotate from near E-W to NNW-SSE in the western region of the southern part of the NSB, gradually from south to north.

In the diagrams of the eastern region of the southern part of the NSB, directions of

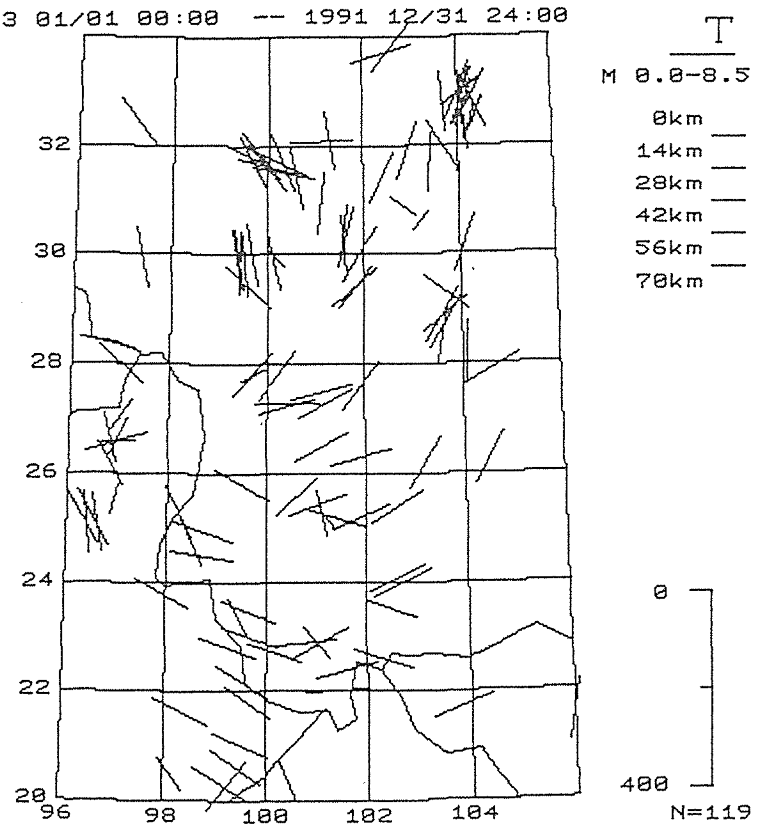

Fig. 4. Distribution of T-axes of the mechanism solutions of 119 earthquakes. It shows the different direction distributions in the western region and eastern region of the southern part of the NSB.

P- and T-axes shown in Fig. 7 are generally different from those in the western region. Five events in the border between Myanmar and Vietnam are included in the subregion E1. In the subregion E1, there are horizontal P-axes in the NNW-SSE direction, horizontal T-axes in the ENE-WSW direction and vertical N-axes. The diagram of the subregion E2 located in the eastern part of Yunnan province is similar to that of the subregion E1. In the subregion E3 (the western part of Sichuan province), there are horizontal P-axes in the WNW-ESE direction, horizontal T-axes in the NNE-SSW direction and the vertical N-axes. The directions of P-axes and T-axes in the subregion E3 display the characteristics that they rotate about 30° counterclockwise relatively to those in subregion E2. The subregion E4 is located in the Songpang-Pingwu area of Sichuan province where many large earthquakes occurred recently. The diagram of the subregion E4 in Fig. 7 means that there is the similar direction of stress field as that in the subregion E3. It can be seen in Fig. 7 that the direction of P-axes rotate from the NNW-SSE to the WNW-ESE direction (from E1 to E4 region) and the average direction of axes is near the E-W direction in the Songpang-Pingwu region. T-axes from south to north also gradually rotate from E-W to NNE-SSW in the eastern

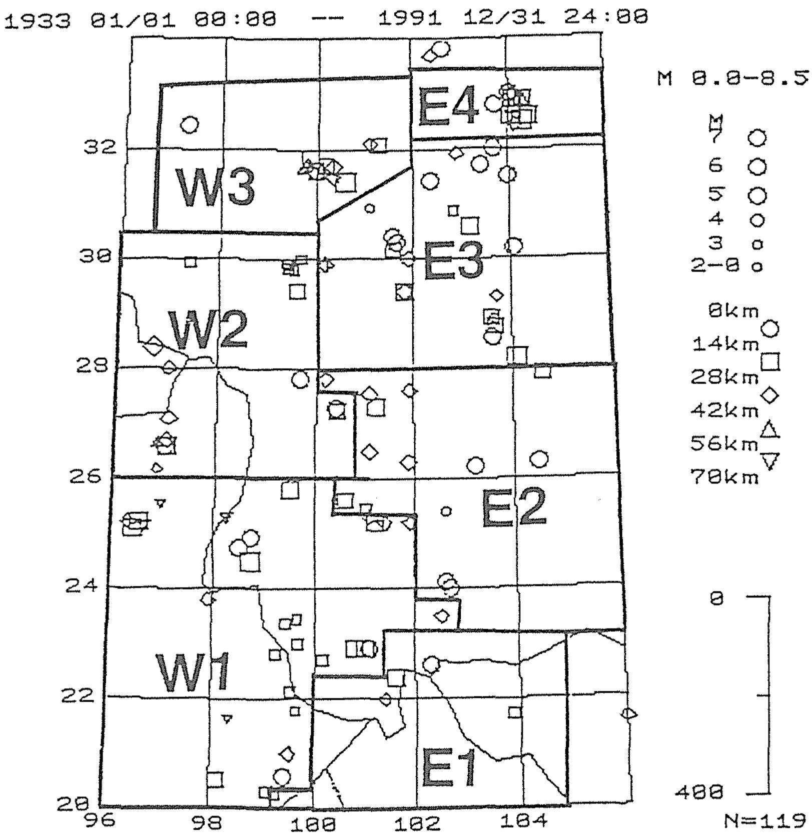

Fig. 5. Distribution of the subregions From south to north, they are the subregions W1, W2 and W3 in the western region and the subregions E1, E2, E3 and E4 in the eastern region.

region from the subregion E1 to the subregion E4. Almost all earthquakes in the subregions E1, E2, E3 and E4 are the strike-slip fault type, except only two earthquakes cases in the subregion E4, which are reverse faulting type.

Based on the mechanism solutions, average directions of P-axes in seven subregions were calculated and shown in Fig. 8. In the western region, the average directions are N37°E, N39°E and N52°E in the subregion W1, W2 and W3, respectively. In the eastern region, they are N25°W, N37°W, N63°W and N64°W in the subregion E1, E2, E3 and E4, respectively. From this distribution, the rotation of the direction of P-axes from south to north in the western region and in the eastern region are found.

In order to show the characteristics of the variation of directions of P- and T-axes from south to north in the western region and in the eastern region in the southern part of the NSB shown above, the relation between azimuths of P-axes and latitudes of epicenters were shown in Fig. 9. In this figure, 95 mechanism solutions of strike-slip faulting type were used. It is found in Fig. 9 that when the latitudes of epicenter increase, azimuths of P-axes rotate counterclockwise in the western region and clockwise in the eastern region. The rotating tendency of P-axes in the eastern region

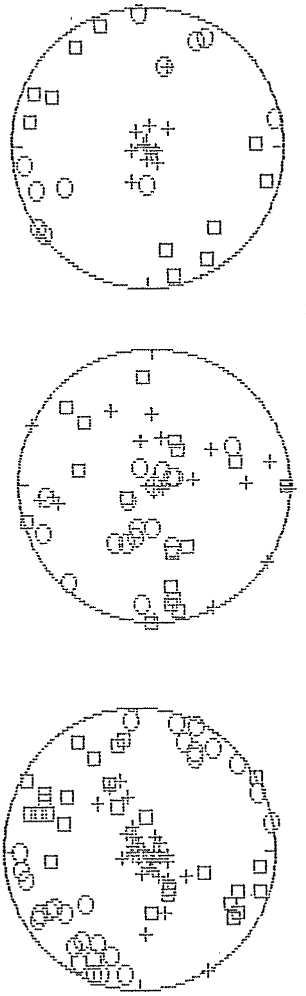

Fig. 6. Projections on the Wulff's nets of lower hemisphere of the P-, T- and N-axes of the mechanism solutions of earthquakes occurred in subregions W1, W2 and W3 located in the western region of the southern part of the NSB. Open circles, squares and crosses show P-, T- and N-axes, respectively.

is clearer than in the western region. It means that the stress field in the western region is controlled by more complex tectonic forces than in the eastern region.

There are complex geological structures and many active strike-slip faults in the southern part of the NSB as shown in Fig. 10. Main faults there are Xianshuihe fault, Longmenshan fault, Anninghe fault, Xiaojiang fault and Red River fault. The Xianshuihe fault (1 in Fig. 10) is a large-scale and typical strike-slip active fault. The trend of this fault is NW-SE along the northeastern border of the Tibetan plateau. Many large earthquakes occurred along this fault, for example, the 1973 Luhuo earthquake (M=7.9). Based on the regional feature of mechanism solutions as mentioned above, the northwestern segment and the southeastern segment of the

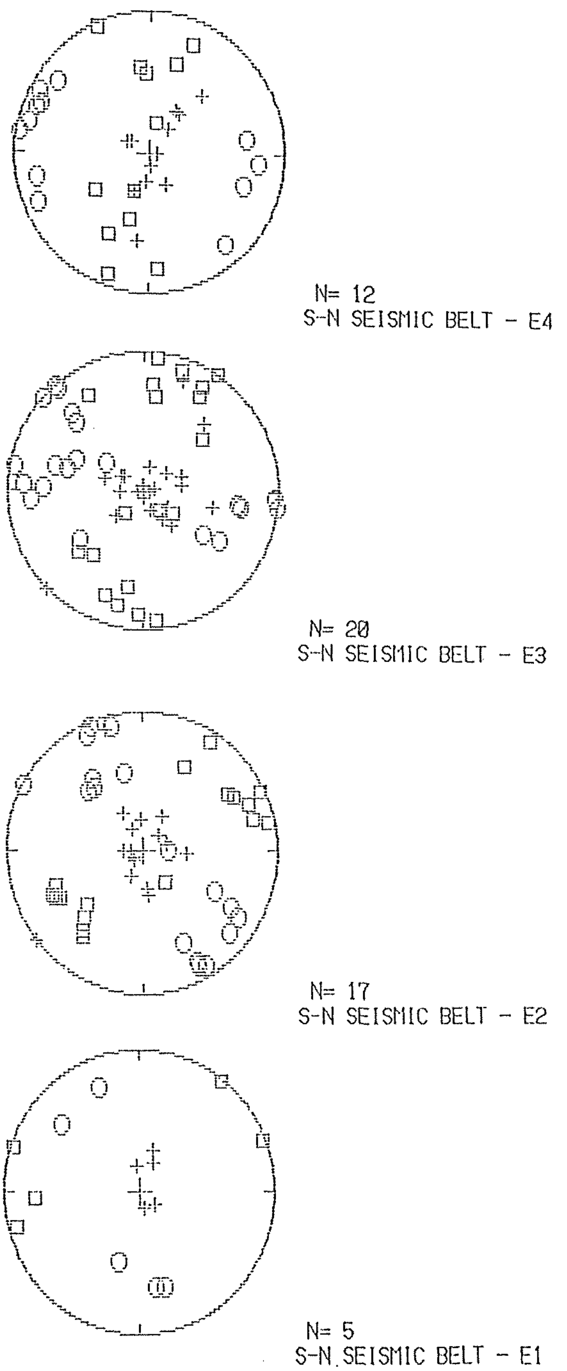

Fig. 7. Projections on the Wulff's nets of lower hemisphere of the P-, T- and N-axes of the mechanism solutions of earthquakes occurred in subregions E1, E2, E3 and E4 located in the eastern region of the southern part of the NSB. The open circles, squares and crosses show P-, T- and N-axes, respectively.

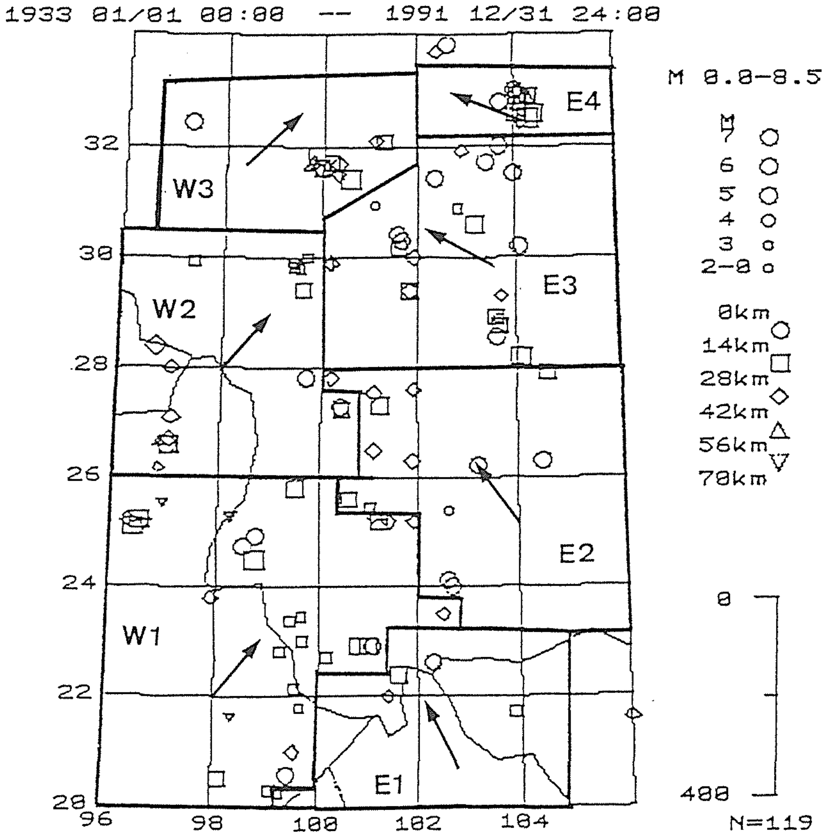

Fig. 8. Average directions of P-axes in seven subregions in the southern part of the NSB.

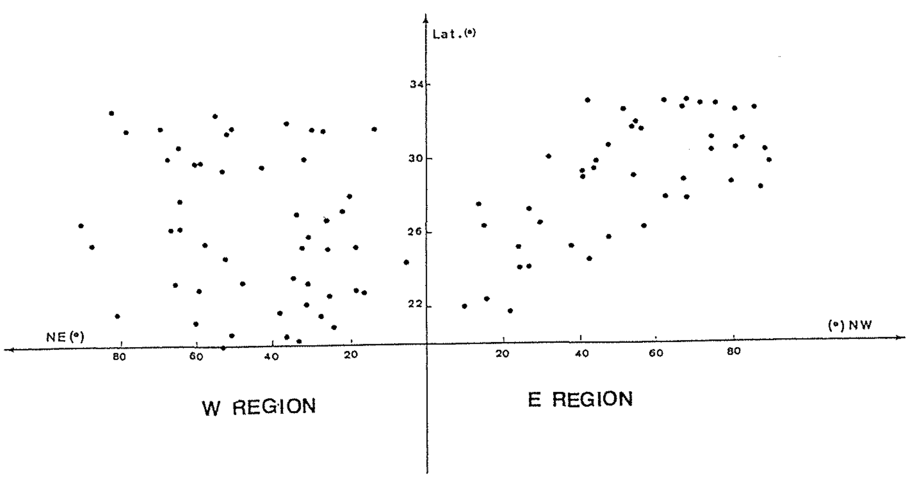

Fig. 9. The relation between azimuths of P-axes and latitudes of epicenters. Here 95 mechanism solutions of strike-slip faulting type were used. The abscissa means azimuths of P-axes of mechanism solutions and the ordinate means latitudes of epicenters. The abscissa means azimuth from north to west in the right (in the eastern region) and azimuth from north to east in the left (in the western region), respectively.

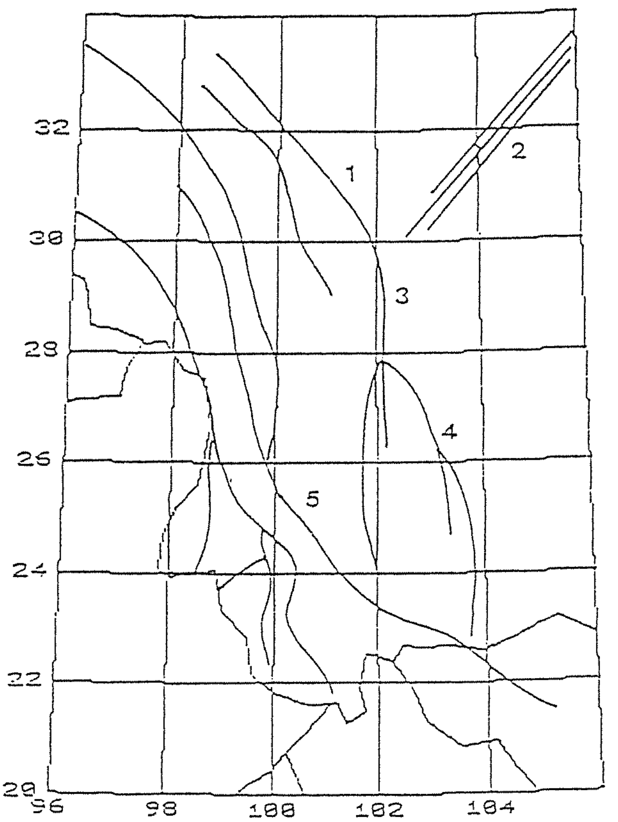

Fig. 10. Distribution of main active faults in the southern part of the NSB. 1; Xianshuihe fault, 2; Longmenshan fault, 3; Anninghe fault, 4; Xiaojiang fault and 5; Red River fault.

Xianshuihe fault belong to the subregion W3 and the subregion E3, respectively. It corresponds to the fact that there are different features of the stress field in two segments along this fault. In order to confirm this difference, mechanism solutions of earthquakes occurred in the two segments of the Xianshuihe fault were investigated in detail. Fig. 11 and Fig. 12 show the Wulff's net projections of lower hemisphere of mechanism solution of each earthquake occurred in the Gangzi and Kangding regions, which are near to the border between two segments and belong to the northwestern segment and to the southwestern segment, respectively. The focal mechanism solutions of 6 events in Fig. 11 show that they are the strike-slip faulting type events. P-axes are in the NE-SW and the E-W directions, T-axes are in the NW-SE and N-S directions there, respectively. Fig. 12 shows that the earthquakes occurred in the southeastern segment are strike-slip faulting type, but directions of P- and T-axes are different with those in the northeastern segment. P-axes are in the NW-SE and the NNE-SSW direction, T-axes are in the NE-SW and ESE-WNW, respectively. Although the two segments are located along the Xianshuihe fault and the distance between them is only about 200 km, there is the difference of the direction of the stress axes. The results obtained in this paper are consistent with the geological and

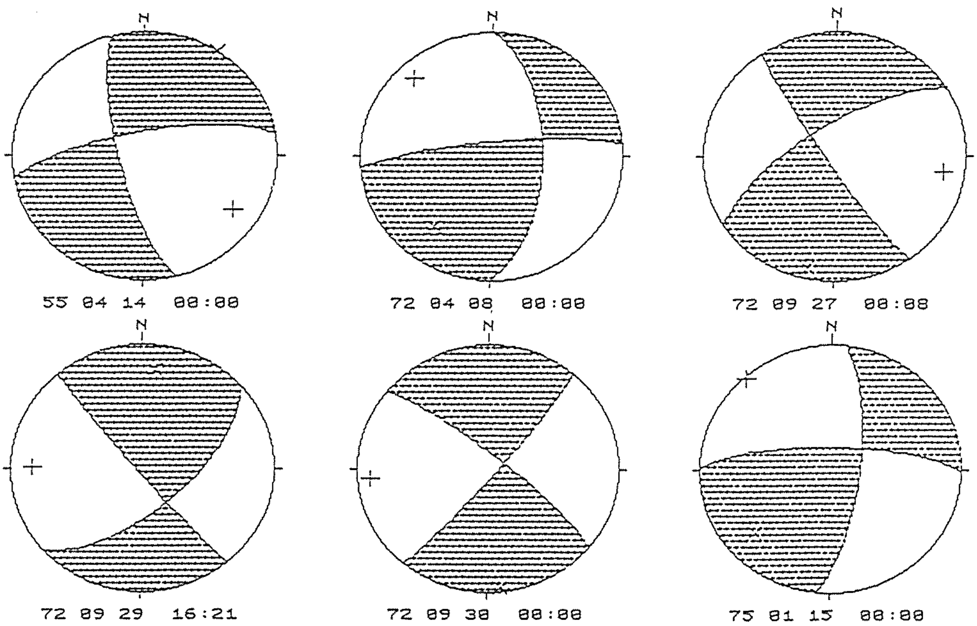

Fig. 11. Projections on the Wulff's nets of lower hemisphere of the P-, T- and N-axes of the mechanism solutions of 6 earthquakes occurred in the Gangzi region located in the northeast to the Daofu region, which is the border between the northwestern and southeastern parts of the Xianshuihe fault.

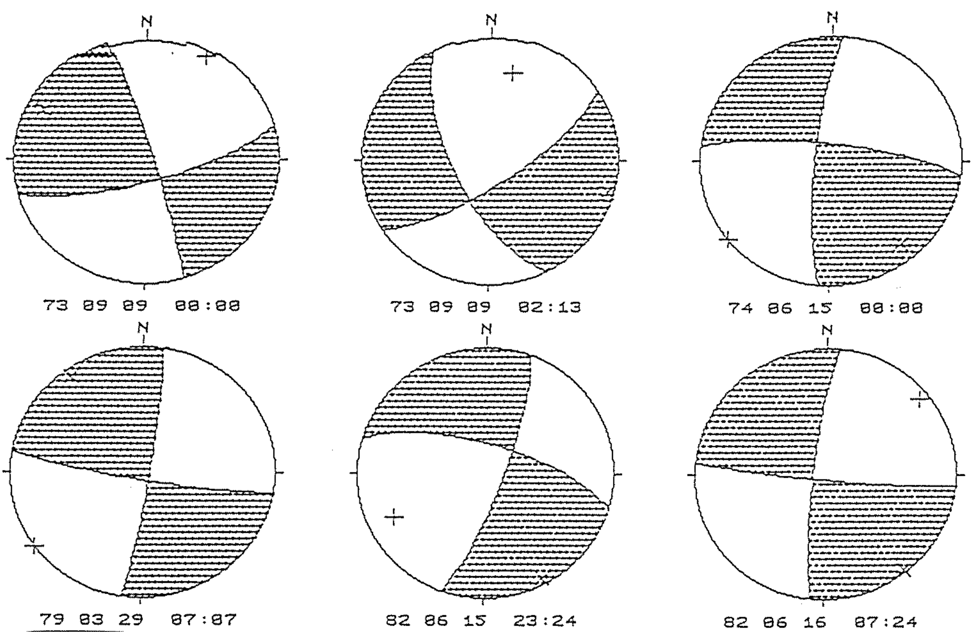

Fig. 12. Projections on the Wulff's nets of lower hemisphere of the P-, T- and N-axes of the mechanism solutioins of 6 earthquaked occurred in the Kangding region located in the southwest to the Daofu region, which is the border between the northwestern and southeastern parts of the Xianshuihe fault.

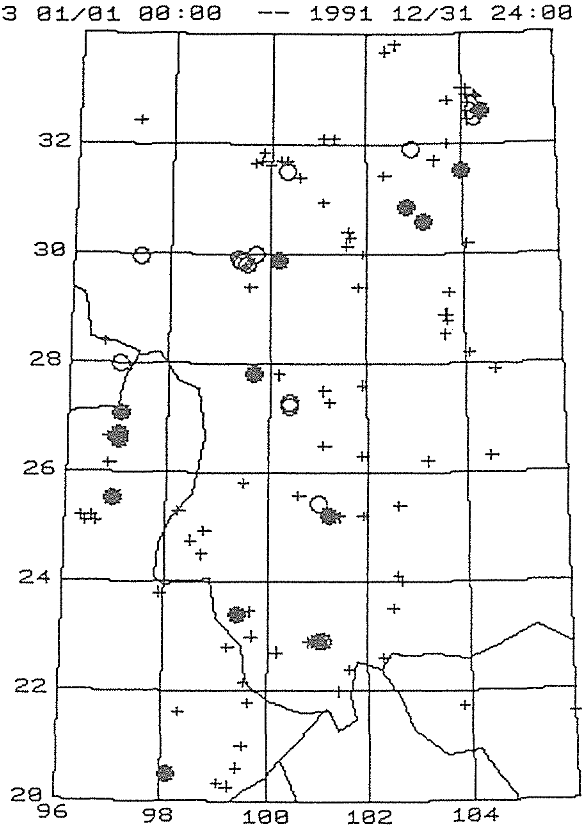

Fig. 13. Distribution of the earthquakes with normal faulting type (open circles), reverse faulting type (closed circles) and the strike-slip faulting type (crosses) in the southern part of the NSB.

geomorphological evidences and the results of the measurement of crustal stresses (Huang et al., 1986, Jiang et al., 1986).

Fig. 13 shows the distribution of the normal, reverse and strike-slip faulting type earthquakes in the southern part of the NSB. Open circles, closed circles and crosses in Fig. 13 show the normal, the reverse and the strike-slip faulting events, respectively. In Fig. 13, in the case that the plunge of P-axis is larger than that of T-axis and it is equal too or more than 45°, the earthpqake is regarded as a normal faulting type event. In the case that plunge angle of T-axis is larger than that of P-axis and equal to or more than 45°, the earthquake is regarded as a reverse faulting type event. In the case that both plunge angle of P- and T-axis are less than 45°, the earthquake is classified into the strike-slip faulting type. As shown in Fig. 13, almost all earthquakes are strike-slip faulting events in the southern part of the NSB except in the subregion W2. 11 normal faulting earthquakes of all 17 earthquakes are predominant in the subregion W2.

4. Discussion

The southern part of the NSB analyzed in the present study was generally regarded as a seismic zone. However, its earthquake-genetating stress field is divided into two seismic regions with respect to characteristics of the stress field obtained in the present analysis.

The earthquake-generating stress field in the continental part of China were analyzed from temporal variations of the seismic activity (Zhao et al., 1990). The temporal variations of the seismicity in the southern part of the NSB do not synchronize with any one of its neighboring seismic zones in the continental part of China. The seismic activitiy here is not related to any unitary plate movement, but is related to the tectonic forces due to the motions of all plates around East Asia.

The velocity structure of the crust in the western region of the southern part of the NSB is different from that in the eastern region according to results of the analysis of group velocities of Rayleigh waves (Li et al., 1989). The velocity structure feature in the western region is mainly similar to those in Tibetan plateau. Therefore, the western region of the southern part of the NSB is regarded as an active seismic region as the Tibetan plateau. The velocity structure feature in the western region is similar to those in South China. According to the velocity structure feature in the crust, the eastern region of the southern part of the NSB is regarded as the subactive region as the South China.

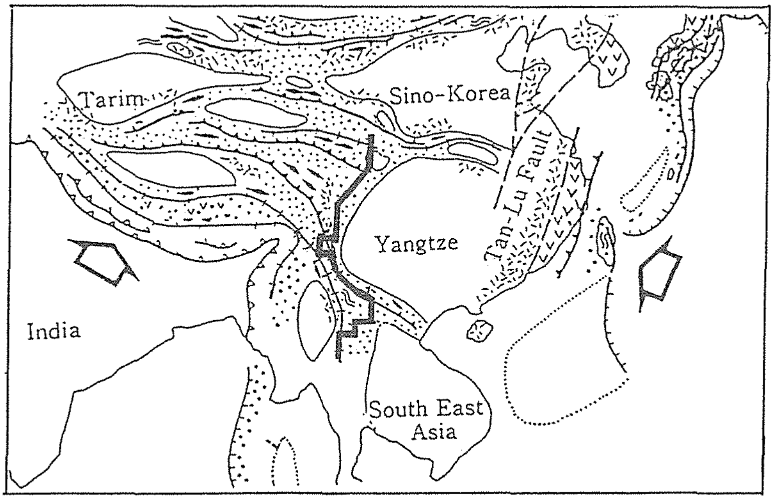

Fig. 14. Distribution of collision zones, subduction zones, main crustal blocks and faults in East Asia. An arrow in the western side shows the relative movement direction of the Indo-Australian plate toward the Eurasian plate. Another arrow in the eastern side shows the relative movement direction of the Philippine Sea plate toward the Eurasian plate. The thick line is the boundary between the western region and the eastern region of the southern part of the NSB of China. This line is consistent with the western border of the Yangtze crustal block and the South East Asia block.

The trend of the boundary between the western and eastern regions obtained in this study is not identical with the trend of all faults in the southern part. Only in the middle part from 23°N to 30.5°N the boundary trend is partly consistent with that of the Red River fault (see Fig. 5 and Fig. 10), especially in the southern part along Ailaoshan mountain. Fig. 14 is a geological tectonic map showing the outline of distribution of collision zones, subduction zones, main faults crustal blocks and so on in East Asia. The boundary between the western and eastern regions of the southern part of the NSB obtained in this paper is also shown in Fig. 14. This boundary is identical with the border between the Yangtze crustal block and the Tibetan Plateau crustal block.

According to geological structure feature, there is a important fault along Ailaoshan mountain, which is a boundary between geosyncline in West China and platform in South China (Li, 1981). The study of the three dimensional velocity tomography of the crust and upper mantle beneath the southern part of the NSB (Liu et al., 1989) suggested that the Yangtze crustal block bordered by Ailaoshan mountain fold belt on the southwest based on results in the depth of 120 km.

Based on the direction tendency of P- and T-axes of earthquakes, the continental area of China is divided three large seismic active regions, West China, North China and South China (Xu et al., 1989). The NSB is the boundary between West China and the eastern part of China including North China and South China. The southern part of the NSB is the boundary between West China and South China. Based on the direction tendency of P- and T-axes, the stress field in the western region of the southern part of the NSB is consistent with that in West China. It is because that the Indo-Australian plate moving northeastward collides to the Eurasian plate in the Himalayan collision zone (Ni & Barazangi, 1984, Chen & Morlnar, 1990). The tectonic force is so strong that it is transmitted northeastward from the collision zone through the West China to the western region of the southern part of the NSB. It controls the earthquake-generating stress field in this wide area. Tibetan plateau moving northwestward encountered with the Yangtze block in the southern part of NSB. If the Yangtze block would only play a role of obstruction, the direction of stress field in the margin of the Yangtze block (South China) due to the extrusion by Tibetan plateau should be oriented in the NE-SW direction consistent with that of the movement of Tibetan plateau. P-axes and T-axes in the eastern region of the southern part of the NSB are in the NW-SE and the NE-SW directions nearly same as those in South China (Xu et al., 1989). It implied that stress field in the eastern region of the southern part of the NSB is different from that in the western region, which comes from South China. The Philippine Sea plate encountered with the Eurasian plate in the Coastal Range in the Taiwan region and the Ryukyu trench. The tectonic force is transmitted from collision zone between the Eurasian plate and the Philippine Sea plate at Taiwan region (Kao & Chen, 1991) through Yangtze block to the eastern region of the southern part of the NSB.

Tectonic forces in the western region and the eastern region with respective dynamic source transmitted from two plates crossed in the southern part of the NSB and control stress field there. The different stress field patterns have been formed within its western and eastern regions, respectively. It is named as the stress field with the

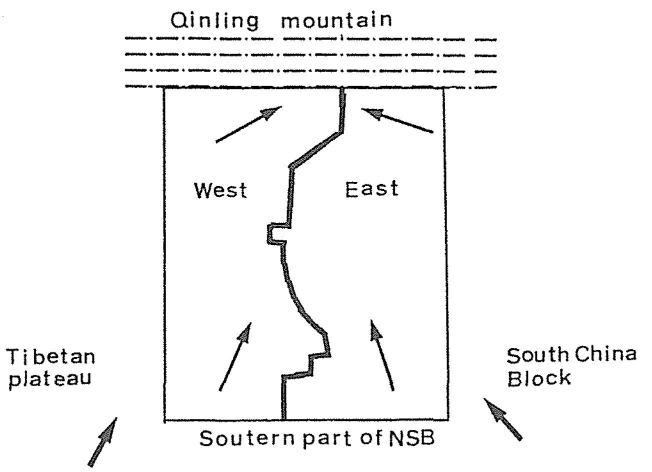

Fig. 15. The model of the geodynamics in and around the southern part of NSB. Thick solid line show the boundary between the western part and the eastern part of the NSB. Arrows with thick lines in the western side and the eastern side show the relative movement directions of the Tibetan plateau and the Yangtze crustal block (South China block) toward the southern part of the NSB. Four thin arrows indicate the directions of P-axes in northern and southern subregions in the eastern region and the western region of the southern part of the NSB, respectively.

pattern of reversal "V" in the southern part of NSB in the present analysis.

As shown as Fig. 8, there are the direction rotations of P- and T-axes from south to north in the western region and the eastern region. In the southern subregions, they may be caused by the mutual northward motions of the Yangtze block and the Tibetan plateau, which reduces the E-W components and strengthens the N-S components. In the northern subregions, Qinling mountains as a large-scale latitudinal structure changes the direction of regional stress field. The model of dynamics in the region is explained as shown in Fig. 15.

5. Conclusions

(1) There is a systematic distribution of the directions of P- and T-axes in the western region and the eastern region of the southern part of the NSB, respectively. P-axes are in the NE-SE direction and T-axes are in the NW-SE direction in the western region. P-axes are in the NW-SE direction and T-axes are in the NE-SW direction in the eastern region, respectively. The average directions of P-axes there show a reversl "V". The boundary between them coincides with that between the Tibetan plateau and the Yangtze crustal block. It can be suggested that the tectonic forces from the Himalayan collision zone between the Indo-Australian and the Eurasian plates and from the collision zone in Taiwan between the Philippine Sea and the Eurasian plates have crossed in the southern part of the NSB and control stress field there.

(2) There are the direction rotations of the P- and T-axes from south to north in the western region and the eastern region in the southern part of the NSB. The mutual

northward motions of the Yangtze block and the Tibetan plateau in the southern subregioins reduce the E-W components and strength the N-S components. In the northern subregions, Qinling mountains change the direction of regional stress field.

(3) The southern part of the NSB is a shallow earthquake zone where most earthquakes are caused by the strike-slip faulting events. The horizontal P- and T-axes dominate the stress field there.

Acknowledgment

The author is very grateful to professor K. Oike for his encouragements for this study and critically reading the manuscript. I express my thanks Mr. Y. Ishikawa and Dr. K. Matsumura for providing valuable data and their kind helps. I also wish to thank Dr. K. Kuge and Dr. Z. Zhao for their useful discussions. Data processing was carried out using FACOM M340R of the Information Data Processing Center for Disaster Prevention Research, Disaster Prevention Research Institute, Kyoto University.

References

Chen, W.P. and P. Molnar, Source parameters of earthquakes and intraplate deformation beneath the Shillong plateau and the northern Indoburman renges, *J. Geophys. Res.*, **95**, 12527–12552, 1990.

Daira, A, The formation of the Japanese Islands — It's history and present as a mobile belt. In : A., Daira and Hagamura, I. (Editors). Tokyo, Illustration, 1986 (in Japanese).

Dziewonski, A.M. and J.H. Woodhouse, An experiment in systematic study of global seismicity : centroid-moment tensor solutions for 201 moderate and large earthquakes of 1981, *J. geophys. Res.*, **88**, 3247–3271, 1983 (a).

Dziewonski, A.M., A. Friedman, D. Giardini and J.H. Woodhouse, Global seimicity of 1982 : centroid-moment tensor solutions for 308 earthquakes, *Phys. Earth Planet. Inter.*, **33**, 76–90, 1983 (b).

Dziewonski, A.M., A. Friedman and J.H. Woodhouse, Centroid-moment tensor solutions for January-March 1983, *Phys. Earth Planet. Inter.*, **33**, 71–75, 1983 (c).

Dziewonski, A.M., A. Friedman and J.H. Woodhouse, Centroid-moment tensor solutions for April-June, 1984, *Phys. Earth Planet. Inter.*, **37**, 87–96, 1985 (a).

Dziewonski, A.M., A. Friedman and J.H. Woodhouse, Centroid-moment tensor solutions for October-December, 1984, *Phys. Earth Planet. Inter.*, **39**, 147–156, 1985 (b).

Dziewonski, A.M., A. Friedman and J.H. Woodhouse, Centroid-moment tensor solutions for April-June, 1985, *Phys. Earth Planet. Inter.*, **41**, 215–224, 1986 (a).

Dziewonski, A.M., A. Friedman and J.H. Woodhouse, Centroid-moment tensor solutions for July-September, 1986, *Phys. Earth Planet. Inter.*, **42**, 205–214, 1986 (b).

Dziewonski, A.M., G. Ekstrom, J.E. Franzen and J.H. Woodhouse, Centroid-moment tensor solutions for January-March 1986, *Phys. Earth Planet. Inter.*, **45**, 1–10, 1987 (a).

Dziewonski, A.M., G. Ekstrom, J.E. Franzen and J.H. Woodhouse, Centroid-moment tensor solutions for October-December 1986, *Phys. Earth Planet. Inter.*, **48**, 5–17, 1987 (b).

Dziewonski, A.M., G. Ekstrom, J.H. Woodhouse and J.E. Franzen, Centroid-moment tensor solutions for July-September 1988, *Phys. Earth Planet. Inter.*, **56**, 165–180, 1989 (a).

Dziewonski, A.M., G. Ekstrom, J.H. Woodhouse and J.E. Franzen, Centroid-moment tensor solutions for October-December 1988, *Phys. Earth Planet. Inter.*, **57**, 179–191, 1989 (b).

Dziewonski, A.M., G. Ekstrom, J.H. Woodhouse and J.E. Franzen, Centroid-moment tensor solutions for January-March, 1989, *Phys. Earth Planet. Inter.*, **59**, 233–242, 1990 (a).

Dziewonski, A.M., G. Ekstrom, J.H. Woodhouse and J.E. Franzen, Centroid-moment tensor solutions

for April-June 1989, *Phys. Earth Planet. Inter.*, **60**, 243–253, 1990 (b).
Dziewonski, A.M., G. Ekstrom, J.H. Woodhouse and J.E. Franzen, Centroid-moment tensor solutions for July-September 1989, *Phys. Earth Planet. Inter.*, **62**, 185–193, 1990 (c).
Dziewonski, A.M., G. Ekstrom, J.H. Woodhouse and G. Zwart, Centroid-moment tensor solutions for January-March 1990, *Phys. Earth Planet. Inter.*, **65**, 197–206, 1991.
Editorial Board of the Atlas on the Lithospheric Dynamics of China State Seismological Bureau, Chief Compiler Ma Xingyuan, Lithospheric dynamics map of China and adjacent seas, Geological Publishing House, Beijing, China, 1986.
Huang, X.W., and J. Zhou, The study on the geodynamics of the Xianshuihe fault. Proceedings of the symposium on the seismicity of the Xianshuihe fault, Seismological Press, Beijing, 210–220, 1986 (in Chinese).
Jiang, N.Q., Z.L. Luo and D.X. Long, The preliminary study on structure stress field and the future of motion of the Xianshuihe fault. Proceedings of the symposium of the seismicity of the Xianshuihe Fault. Seismological Press, Beijing, 221–237, 1986 (in Chinese).
Kao, H. and W.P. Chen, Earthquakes along the RyuKyu-Kyushu arc: Strain segmentation, lateral compression, and the thermomechanical state of plate interface, *J. Geophys. Res.*, **96**, B13, 21443–21485, 1991.
Kan, R.J., S.C. Zhang, F.T. Yan and L.S. Yu, Present tectonic stress field and its relation to the characteristics of recent tectonic activity in Southwestern China, *Acta Geophysica Sinica,* Vol. 20, No. 2, 96–109, 1977 (in Chinese).
Li, B.J., N. Li and H. Chen, Group velocity differences of Rayleigh waves between the NS Seismic Belt, China, and tectonic implications, *Acta Seismologica Sinica,* Vol. 11, No. 3, 268–274, 1989 (in Chinese).
Li, S.B., Seismology in China. Seismological Press, Beijing, China, 1981 (in Chinese).
Liu, J.H., F.T. Liu, H. Wu, Q. Li and G. Hu, Three Dimensional velocity images of the crust and upper mantle beneath North-South Zone in China, *Acta Geophysica Sinica,* Vol. 32, No. 2, 143–152, 1989 (in Chinese).
Ni, J., and M. Barazangi, Seismotectonics of the Himalayan collision zone: Geometry of the underthrusting Indian plate beneath the Himalayan, *J. Geophys. Res.*, **89**, B2, 1147–1163, 1984.
Peltzer, G. and P. Tapponnier, Formation and evolution of strike-slip collision: an experimental approach, *J. Geophys. Res.*, **93**, (B12), 15, 085–15, 117, 1988.
Sichuan province Seismological Bureau, The 1933 Diexi earthquake, Sichuan Province Scientific and Technological Press. Chengdu, China, 1983 (in chinese).
Sung, Z.H., C.G. An, C.Y. Wang, L.J. Zhang and Z.R. Qiu, The P wave velocity of upper mantle beneath Qinghai-Tibet plateau and North-South Seismic Zone, *Acta Geophysica Sinica,* Vol. 28, Supp.I, 148–160, 1985 (in Chinese).
Wang, Z.S., Z.Y. Wang, J.P. Gu and X.Y. Xiong, A preliminary investigation of the limits and certain features of the North-South Seismic Zone of China, *Acta Geophysica Sinica,* Vol. 19, No. 2, 110–117, 1976 (in Chinese).
Xu, J.T, Brief account of Xiaojin earthquake in Sichuan province. *Recent developments in world seismology,* 7, 7–10, 1991 (in Chinese).
Xu, J.T, Damages caused by the Xiaojin M 5.2 earthquake of Feb. 18, 1991 and countermeasures. *Recent developments in world seismology,* 12, 7–11, 1991 (in Chinese).
Xu, J.R., Z.X. Zhao, Y. Ishikawa and K. Oike, Regional characteristics of focal mechanisms of shallow earthquakes in and around China. Proceeding of the Japan-China (Taipei) Joint Seminar on Natural Hazard Mitigation, 41–49, 1989.
Xu, Z.H., S.Y. Wang, Y.R. Huang, A.J. Gao, X.F. Jin and X.D. Chang, Directions of main stress axes in southwestern China deduced from microearthquake data, *Acta Seismologica Sinica,* Vol. 30, No. 5, 476–486, 1987 (in Chinese).
Zhao, Z.X., K. Matsumura, K. Oike and Y. Ishikawa, Regional characteristics of temporal variation of seismic activity in East Asia and their mutual relations (3) West China and its neighboring regions, *ZISIN,* II, Vol.41, 389–400, 1988 (in Japanese).
Zhao, Z.X., K. Oike, K. Matsumura and Y. Ishikawa, Stress field in the continental part of China derived from temporal variations of seismic activity, *Tectonophysics,* **178**, 357–372, 1990.